

Morphology of the Solar Corona from Radio Occultation Measurements: implications for Solar Probe

Richard WOO

*Jet Propulsion Laboratory
California Institute of Technology
Pasadena, CA 91109*

Abstract. While ray-like structures in the solar corona have been observed in white-light coronagraph and solar eclipse images for many years, recent progress using radio occultation measurements have revealed a plethora of structures extending to sizes as small as 1 km - three orders of magnitude smaller than those observed in white-light and eclipse measurements. Advances have also been made in understanding the variation of large- and small-scale structures in the extended corona and their organization by the heliospheric current sheet. This paper summarizes the latest results on the morphology of the near-Sun solar wind obtained from radio occultation measurements, and their impact on the planning and conduct of a mission to the Sun such as Solar Probe.

INTRODUCTION

In planetary exploration, radio occultation measurements carried out with spacecraft radio signals have usually provided the first definitive global measurements of planetary atmospheres that would set the stage for follow-on missions to observe the atmosphere directly. Examples of this are the radio occultation measurements of Venus by the Mariner 5 fly-by mission [1] that preceded the *in situ* measurements by the Pioneer Venus probes [2], and the Pioneer 10 radio occultation measurements of Jupiter [3] before the Galileo Probe mission [4]. Radio occultation measurements of the solar corona using both spacecraft signals and natural radio sources would be expected to serve the same purpose for a mission to the Sun such as Solar Probe.

Compared with the measurements of planetary atmospheres, radio occultation measurements of the corona comprise an unusually rich data set because they cover a wider variety of radio propagation phenomena. Conducted for over four decades, they have observed mainly density, density fluctuations, and solar wind velocity. Density has been investigated by ranging measurements [5- 6]; density fluctuations by angular broadening [7], intensity scintillation [8], spectral broadening [9- 10], phase or Doppler scintillation [9-10], and frequency decorrelation measurements [11]; and solar wind speed by multiple-station intensity scintillation measurements - often referred to as 11'S for interplanetary scintillation [12- 13].

Despite extensive observations, the potential of radio occultation measurements for defining the global morphology of the near-Sun solar wind and paving the way for a mission to the Sun has not been realized until now. The purpose of this paper is to review recent advances in the morphology of the solar corona, their implications for the basis and conduct of scientific exploration of the near-Sun solar wind by Solar Probe, and their implications for prediction of adverse scintillation effects on the Solar Probe communications link.

MORPHOLOGY OF THE SOLAR CORONA

A major surprise has been the pervasion of ray-like structures found in the corona [14-16]. The finest structures measure about 1 km across at the Sun (see illustration in Fig.1) - three orders of magnitude smaller than the smallest filamentary structures seen in X-ray, UV, EUV and visible white-light images [17-21]. Quasi-stationary small-scale structures in the corona were first identified by the similarity in Doppler scintillation measurements (reflecting variations in the time derivative of path-integrated electron density) of a coronal streamer over two successive solar rotations [14].

Evidence for the finest structures of 1 km (flux tubes) include: (1) the break near 1 Hz in the power spectrum of the temporal variations of path-integrated density observed in phase scintillation measurements, marking the separation between the low-frequency density variations due to structures and high-frequency variations due to convected small-scale turbulence, and (2) the high anisotropy in angular broadening measurements indicating scattering that is stronger transverse to the magnetic field than along it [15]. The spatial information on density fluctuations in the plane of the sky provided by angular broadening measurements is crucial in showing that the break in the density spectrum does not correspond to a spatial scale

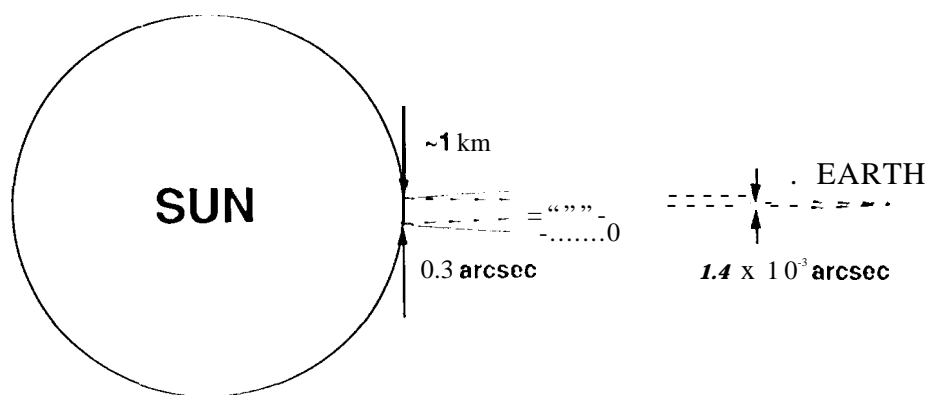


Figure 1. Depiction of finest coronal structure which is 1 km at the Sun. Viewed from the Sun, the radially expanding structure has an angular size of 0.3 arcsec. From Earth, the angular size of the 1-km structure is 1.4×10^{-3} arcsec.

in the flow direction of the solar wind, as it would in the case of convected turbulence [9- 10], but rather to a spatial scale transverse to the magnetic field (flux tube size).

Early investigations of the global variations of the plasma properties based on radio occultation measurements have concentrated on the dependence on heliocentric distance, latitude, and solar cycle [5-- 11]. Starting with the striking organization of small-scale density fluctuations first noted in Doppler scintillation measurements [22], steady progress has been made in understanding the morphology of the corona, and its relationship to results from white-light coronagraphs [16] and direct spacecraft measurements beyond 0.3 AU [23]. Strongly organized by the large-scale solar magnetic field (heliospheric current sheet or coronal streamers in white-light images), typical profiles of N , AN and v inside $30R_{\odot}$ are depicted schematically in Fig. 2 relative to coronal streamers as seen face on and looking down on the ecliptic plane. The corresponding heliospheric current sheet is hence transverse to the ecliptic plane, and the profiles represent variation with solar longitude. This geometry has been chosen for convenience of illustration, but the profiles apply in general to a plane that is transverse to the heliospheric current sheet as found in the case of white-light measurements of the inner corona [14]. Path-integrated electron density N represents the large-scale structure; fluctuations in path-integrated density AN reflect small-scale structures when the sampling rates are high, e.g., small-scale structures with sizes of 20–240 km for 3-min Doppler scintillation [14]; AN/N is fractional path-integrated density fluctuations; v is solar wind velocity.

The profile of N near the Sun is similar to that observed by white-light measurements of polarization brightness (also measuring path-integrated density) at $4R_{\odot}$ [24], indicating that the large-scale structure of the heliospheric current sheet changes little as it extends into interplanetary space near the Sun. The angular thickness (full width at half maximum) of the heliospheric current sheet is about 20° , and the drop in N across the heliospheric current sheet from its peak is a factor of 2-4.

Higher spatial resolution of N is achieved by increasing the sampling rate of the ranging or Doppler measurements [16]. When this is done, the profile of N does not change significantly because AN is only a small percentage (several %) of N . However, when the background large-scale structure is removed, the profile of the small-scale structures AN is more dramatic than that of N . The masking of small-scale structures also occurs in white-light images where they are revealed only if the images are processed to enhance density gradients [19,24]. Whereas the angular thickness of the heliospheric current sheet in terms of N is about 20° , it is only a few degrees for AN , because the small-scale structures are confined to narrow regions comprising the stalks (extensions, tips) of the coronal streamers. Not only are the small-scale structures more striking because they occupy smaller regions, but also because the rise in AN is much higher than that in N - an order of magnitude or more in the case of AN vs a factor of 2-4 in the case of N . Only one enhancement in AN is shown in Fig. 2, but sometimes more than one is observed, which may represent multiple current sheets [25]. Recent studies based on density spectra also show that the finest filamentary structures are a factor of three smaller within the extensions of

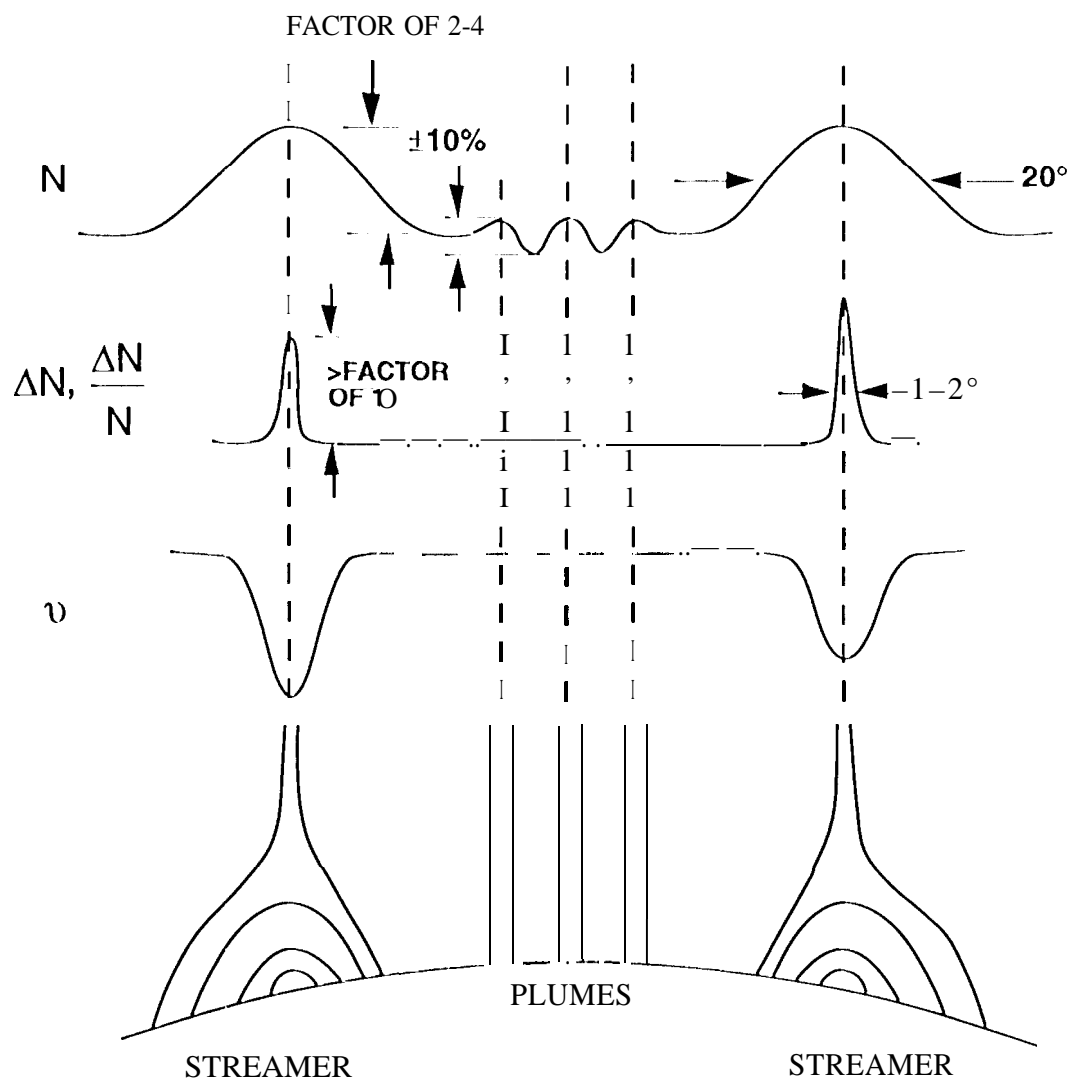


Figure 2. Schematic of profiles of path-integrated density N , fluctuations of path-integrated density ΔN , fractional path-integrated density fluctuations $\Delta N/N$, and solar wind velocity v . The two coronal streamers are observed face-on looking down on the ecliptic plane. In this view the heliospheric current sheet is normal to the plane of the figure. The profiles apply to the stalks or extensions of coronal streamers observed in white-light pictures beyond several solar radii. Several plumes are also shown in the fast wind far from the heliospheric current sheet and between the two streamers.

coronal streamers than in coronal holes [26]. Although AN has often been assumed to be proportional to N and hence a measure of N [27-28], simultaneous scintillation and ranging measurements have shown that N is not constant, but varies similarly as AN across the streamer [14,29]. For this reason, the profiles of AN and AN/N are shown as one in Fig. 2.

Ranging measurements of large-scale density structure show that plumes are not exclusive to polar coronal holes, but appear in all regions away from the heliospheric current sheet, including those at low latitude [30]. Moreover, these plumes extend far into interplanetary space, having been detected in ranging measurements at least as far as 401 AU. A few plumes, which typically exhibit a peak-to-peak variation in N of about $\pm 10\%$ are depicted between the streamers in Fig. 2.

Multiple-station intensity scintillation measurements (IPS) complement path-integrated measurements of density N by providing estimates of solar wind velocity v. However, there are some major differences between the measurements of N and v. With ranging and Doppler measurements, N is observed directly (without inversion). Moreover, both white-light images of path-integrated density and angular broadening measurements confirm that spatial structures are indeed observed in the ranging and Doppler measurements of N [15, 16]. In contrast, v is not an observable of path-integrated velocity, but is instead an estimate of velocity inferred from 11'S measurements and dependent on solar wind models [31]. While absolute velocity estimates are more sensitive to modeling, the relative changes are less so. The temporal resolution of 11'S measurements is limited by the minimum observation time needed to obtain accurate estimates of velocity, leading to a spatial resolution for the structured corona that is generally significantly coarser than that of ranging or Doppler measurements. In spite of these shortcomings, velocity estimates deduced from 11'S measurements inside 12 R_s using the VLA in 1983 [32] show that the wind appears relatively steady over coronal holes, but exhibits large gradients over the streamer belt [33], similar in character to the velocities observed by Ulysses much farther out [34]. "There is growing evidence that the sources of the slow solar wind are more localized nearer the Sun [12,35], and that they coincide with the stalks or extensions of the coronal streamers where enhanced AN is observed. Velocity profiles reflecting these results are shown in Fig. 2. Although no variation is shown across the plumes, velocity estimates deduced from the 1983 VLA measurements [32] and covering an angular extent of 4.4° over a low-latitude coronal hole hints at a systematic variation of $\pm 10\%$ (see Fig. 2 of [33]) that may represent the spatial variation across a coronal plume. If conservation of mass flux holds, then the 3.1070 variations of velocity and density would be anti-correlated.

Finally, another significant result based on 11'S estimates of velocity, which has an impact on the planned plasma measurements of Solar Probe, is the recent finding that the acceleration of the polar wind may be complete by 101 AU [31,36].

IMPLICATIONS FOR SOLAR PROBE

Results from radio occultation measurements indicate that the range and extent of structures in the region of the solar wind that will be observed by Solar Probe is extensive. The flow of plasma is guided by these ubiquitous radially expanding structures that are aligned along the solar magnetic field and rotate with the Sun. These results show that there is a close connection between the Sun and the near-Sun solar wind, and reinforce the importance of conducting both solar imaging and interplanetary measurements with Solar Probe in order to better understand the nature of the connection. The uncertainties in distinguishing spatial and temporal variations with *in situ* plasma measurements [37-39], and the indispensable role of spatial measurements provided by angular broadening measurements in confirming the detection of the finest filamentary structures in phase scintillation measurements, underscore the urgency for imaging the corona when *in situ* measurements are made by Solar Probe.

Doppler scintillation measurements have given us a first look at small-scale structures that may play a role in the heating and acceleration of the solar wind [18,40,41]. The density fluctuations across the stalks of coronal streamers -- the apparent sources of the slow solar wind -- are strikingly higher than those in the fast wind from coronal holes. The low telemetry rates of the Solar Probe mission will severely restrict the sampling rates of the plasma measurements, and it is useful to examine the impact of these limitations.

Shown in Fig. 3 is the trajectory of Solar Probe seen from Earth and broken into three segments designated: (1) early prime mission, (2) critical zone 1, and (3) critical zone 3 [36]. The angular size of the 1 km filamentary structures is 0.3 arcsec, and that of plumes and stalks is 2". For a sampling rate of 100s (currently assumed for the Minimum Solar Minimum mission [36]), the corresponding spatial resolutions for the early prime mission, critical zone 1, and critical zone 3 segments is 0.07°, 0.23°, and 0.64°, respectively. These resolutions may not be adequate for characterizing the plumes, and are certainly inadequate for characterizing the small-scale structures. The resolution in critical zone 2 is especially poor for observing the stalks of coronal streamers. The stalks are interesting not only because they are the apparent sources of the slow solar wind, but also because the abrupt change in the small-scale density structures indicates that there are probably significant changes in other plasma properties as well.

The sampling rates necessary to measure the finest filamentary structures of 0.3 arcsec in the early prime mission, critical zone 1, and critical zone 2 segments would be 9, 28, 77 samples per second, respectively. Even higher rates would be necessary to characterize the turbulence within them. Such sampling rates are obviously too high for the mission's *in situ* measurements, but not for phase/Doppler measurements of path-integrated density [14,16] between Earth and Solar Probe

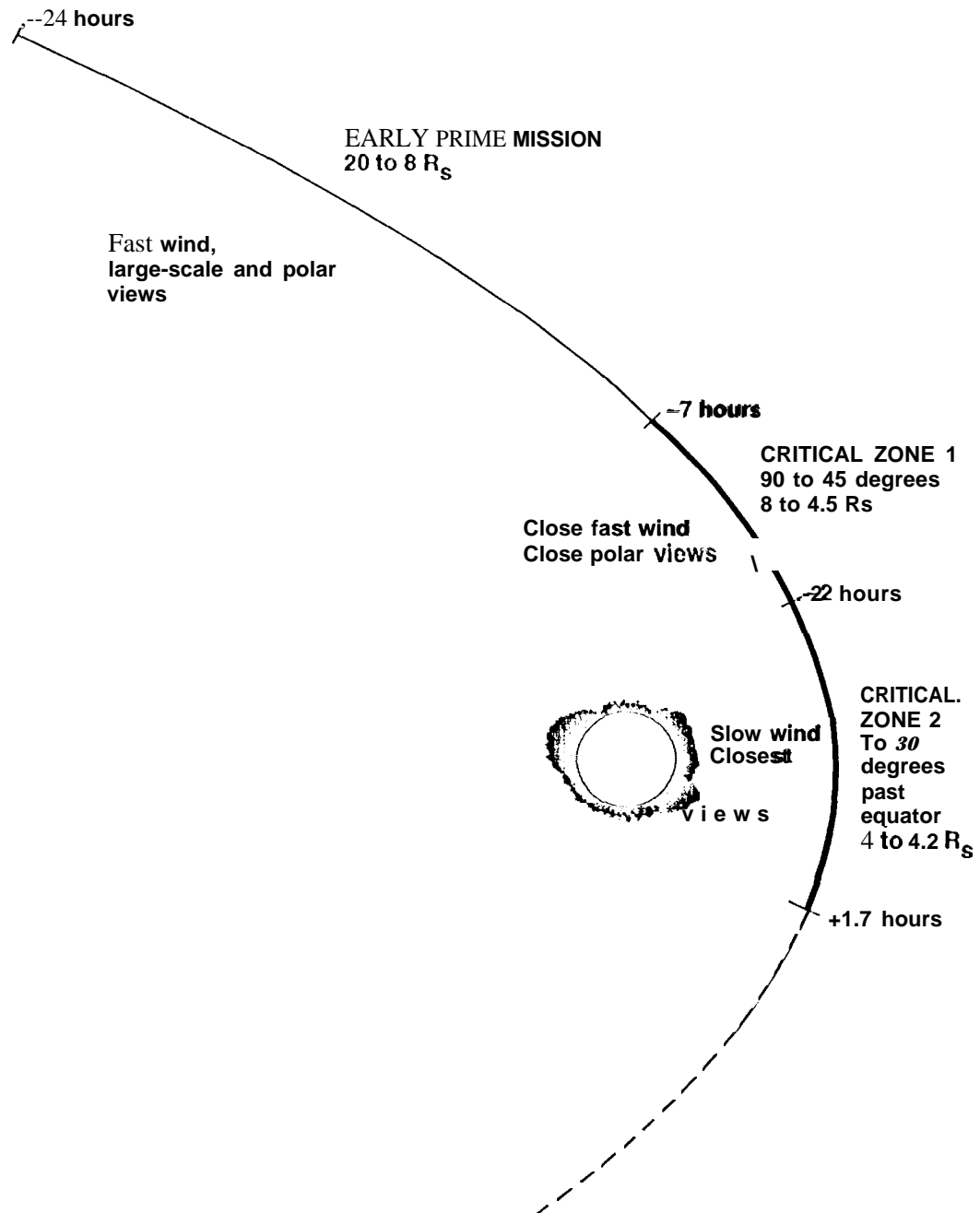


Figure 3. As seen from Earth, the trajectory of the Solar Probe spacecraft is broken down into three segments: (1) early prime mission, (2) critical zone 1, and (3) critical zone 2. The closest approach is at 4 R_S . The corresponding spatial resolutions of the *in situ* Solar Probe plasma measurements for these three periods when the sampling time is 100 s are given in the text.

using the Solar Probe radio link. The Solar Probe communications link will, therefore, also serve as a scientific tool for probing the solar wind, complementing the *in situ* measurements by providing measurements of the small-scale structures,

The same radio scintillation phenomenon, whose observation has made it possible to remotely sense small-scale coronal structures and convected turbulence, degrades and limits the telemetry rate of the Solar Probe communications link [42]. Knowing that the level of scintillation varies in a more systematic (high near the heliospheric current sheet and low away from the current Sheet) rather than random way, as previously thought, leads to lower uncertainties in the scintillation models used in the design of the communications link, and may make it possible to raise telemetry rates. However, while higher telemetry rates could result when probing the high latitude solar wind away from the heliospheric current sheet (early prime mission), the closest approach distance of $4R_s$ occurs at low latitude (critical zone 2), where the scintillation level would not only be highest, but where high telemetry rates would be most needed in order to sample the solar wind plasma fast enough to detect the coronal streamer stalks.

CONCLUSIONS

As a remote sensing tool, the potential of radio occultation measurements for defining the global morphology of the corona that Solar Probe will encounter is finally being realized and benefits are being reaped. An important step in this development has been the demonstration of the relationship between solar wind and solar corona measurements of path-integrated density. Despite the close association, the connection was not understood until now, apparently because of disparity in resolution and viewing geometry. While spatial and temporal resolution are both limited in white-light coronagraph measurements, they are usually much higher in radio measurements of path-integrated density [16,43]; white-light views latitudinal variation best, while the radio measurements probe mainly longitudinal variation, and even this is generally masked by the dominant radial variation [43].

Radio occultation measurements show that the dynamic solar wind is highly structured and closely connected to the Sun. Small-scale structures are ubiquitous, and plumes more pervasive than previously thought. Small-scale structures, which may play a role in heating and acceleration of the solar wind, exhibit strong and abrupt change across the stalks or extensions of coronal streamers. The finest filamentary structure could only be unambiguously identified with spatial measurements. These new results underscore the significance of imaging the Source on the Sun of the solar wind directly observed by Solar Probe, as well as the solar corona along the trajectory of Solar Probe in order to provide context for the *in situ* measurements. Sampling rates and observing strategy that includes on-board processing are important factors to consider if the role of the structures in heating and acceleration of the solar wind and the source of the slow solar wind are to be under-

9. Woo, R. and Armstrong, J. W., *J. Geophys. Res.* 84, 7288 (1979).
10. Coles, W. A., Liu, W., Harmon, J. K., and Martin, C. I., *J. Geophys. Res.* 96, 1745 (1992).
11. Coles, W. A., Grail, R. R., Klinglesmith, M. T., and Bourgois, G., *J. Geophys. Res.* 100, 17069 (1995).
12. Kojima, M. and Kakinuma, T., *Spin? Sci. Rev.* 53, 173 (1990).
13. Rickett, B. J. and Coles, W. A., *J. Geophys. Res.* 96, 1717 (1991).
14. Woo, R., Armstrong, J. W., Bird, M. K., and Pätzold, M., *Astrophys. J.* 449, L91 (1995).
15. Woo, R., *Nature* 379, 321 (1996).
16. Woo, R., in *Solar Wind Eight*, eds. D. Winterhalter, J. Gosling, S. R. Habbal, W. Kurth, and M. Neugebauer, AIP, in press.
17. Bohlin, J. D., Vogel, S. N., Purcell, J. D., Sheeley, Jr., N. R., Tousey, R., and van Hoosier, M. E., *Astrophys. J. Lett.* 197, L133 (1975).
18. Habbal, S. R., *Ann. Geophys.* 10, 34 (1992).
19. Koutchmy, S., *Solar Phys.* 52, 399 (1977).
20. Koutchmy, S. et al., *Astron. Astrophys.* 281, 249 (1994).
21. Guhathakurta, M. and Fisher, R., *Geophys. Res. Lett.* 22, 1841 (1995).
22. Woo, R. and Gazis, J., *Nature* 366, 543 (1993).
23. Huddleston, D. E., Woo, R., and Neugebauer, M., *J. Geophys. Res.* 100, 19951 (1995).
24. Guhathakurta, M., Holzer, T. E., and MacQueen, R. M., *Astrophys. J.* 458, 817 (1996).
25. Crooker, N. U., Siscoe, G. L., Shodhan, S., Webb, D. F., Gosling, J. T., Smith, E. J., *J. Geophys. Res.* 98, 9371 (1993).
26. Woo, R. and Habbal, S. R., *Astrophys. J.*, submitted.
27. Houminer, Z. and Lewish, A., *Planet. Space Sci.* 10, 1041 (1974).
28. Tappin, S. J., *Planet. Space Sci.* 34, 93 (1986).
29. Woo, R., Armstrong, J. W., Bird, M. K., and Pätzold, M., *Geophys. Res. Lett.* 22, 329 (1995).
30. Woo, R., *Astrophys. J.* 464, L95 (1996).
31. Grall, R. R., Colts, W. A., Klinglesmith, M. T., Breen, A. R., Williams, P. J. S., Markkanen, J., and Fisser, R., *Nature* 379, 429 (1996).
32. Armstrong, J. W., Coles, W. A., Kojima, M., and Rickett, B. J., in *The Sun and the Heliosphere in Three Dimensions*, ed. R. Marsden, Dordrecht: Reidel, 1986, pp. 59-64.
33. Woo, R., *Geophys. Res. Lett.* 22, 1393 (1995).
34. Gosling, J. T., et al., *Geophys. Res. Lett.* 22, 3329 (1995).
35. Kojima, M., Washimi, H., Misawa, H., and Hakamada, K., in *Solar Wind Seven*, eds. E. Marsch and R. Schwenn, Oxford: Pergamon Press, 1992, pp. 201-204.
36. *Close Encounter with the Sun*, Report of the Minimum Solar Mission Science Definition Team, JPL 11-12850, August 31, 1995.
37. Thieme, K. M., Marsch, E., and Schwenn, R., *Ann. Geophys.* 8, 713 (1990).

38. Neugebauer, M., Goldstein, B. E., McComas, D. J., Suess, S. T., Balogh, A.,
J. Geophys. Res. **100**, 23389 (1995).
39. McComas, D. J., et al., *J. Geophys. Res.* **100**, 19893 (1995).
40. Dere, K. J., Bartoe, J.-D. F., Brueckner, G. E., Cook, J. W., and Socker, D. G., *Solar
Phys.* 114, 223 (1987).
41. Habbal, S. R., *Space Sci. Rev.*, 70, 37 (1994).
42. Armstrong, J. W., Woo, R., and Koerner, M., paper AIAA-82-0044, AIAA 20th
Aerospace Sciences Meeting Proceedings, January 11-14, 1982, Orlando,
Florida.
43. Woo, R., *Astrophys. J.* 458, 187 (1996).
44. Goldstein, R. M., *Science* 166, 598 (1969).
45. Woo, R., *J. Geophys. Res.* 98, 18999 (1993).